Prostate-specific deletion of the murine Pten tumor suppressor gene leads to metastatic prostate cancer

Shunyou Wang,[1,2] Jing Gao,[1,2] Qunying Lei,[1,2] Nora Rozengurt,[3] Colin Pritchard,[4] Jing Jiao,[1,2] George V. Thomas,[3] Gang Li,[1,2] Pradip Roy-Burman,[5] Peter S. Nelson,[4] Xin Liu,[2,3] and Hong Wu[1,2,*]

[1]Howard Hughes Medical Institute
[2]Department of Molecular and Medical Pharmacology
[3]Department of Pathology and Laboratory Medicine
University of California Los Angeles School of Medicine, Los Angeles, California 90095
[4]Division of Human Biology Mailstop D4-100, Fred Hutchinson Cancer Research Center, 1100 Fairview Avenue, Seattle, Washington 98109
[5]Department of Pathology, Keck School of Medicine, University of Southern California, 2011 Zonal Avenue, Los Angeles, California 90033
*Correspondence: hwu@mednet.ucla.edu

Summary

The murine *Pten* prostate cancer model described in this study recapitulates the disease progression seen in humans: initiation of prostate cancer with prostatic intraepithelial neoplasia (PIN), followed by progression to invasive adenocarcinoma, and subsequent metastasis with defined kinetics. Furthermore, while *Pten* null prostate cancers regress after androgen ablation, they are capable of proliferating in the absence of androgen. Global assessment of molecular changes caused by homozygous *Pten* deletion identified key genes known to be relevant to human prostate cancer, including those "signature" genes associated with human cancer metastasis. This murine prostate cancer model provides a unique tool for both exploring the molecular mechanism underlying prostate cancer and for development of new targeted therapies.

Introduction

Prostate cancer is the most common malignancy in men and the second leading cause of male cancer-related deaths in the Western world. Its development proceeds through a series of defined states, including prostatic intraepithelial neoplasia (PIN), prostate cancer in situ, invasive and metastatic cancer. The standard therapies include androgen ablation that initially causes tumor regression. However, tumor cells will eventually relapse and develop into hormone refractory prostate cancer (HRPC) (Denis and Murphy, 1993; Landis et al., 1999).

The *PTEN* (phosphatase and tensin homolog deleted on chromosome 10) tumor suppressor gene is one of the most frequently mutated/deleted genes in various human cancers (Bose et al., 2002; Deocampo et al., 2003; Sun et al., 2002; Wang et al., 2003; Zhou et al., 2002). Germline mutations in the *PTEN* gene have been associated with Cowden syndrome and related diseases in which patients develop hyperplastic lesions (harmatomas) in multiple organs with increased risks of malignant transformation (Dahia, 2000; Liaw et al., 1997; Marsh et al., 1999). *PTEN* alteration is strongly implicated in prostate cancer development. *PTEN* deletions and/or mutations are found in 30% of primary prostate cancers (Dahia, 2000; Sellers and Sawyers, 2002) and 63% of metastatic prostate tissue samples (Suzuki et al., 1998b), placing *PTEN* mutation among the most common genetic alterations reported in human prostate cancers.

PTEN-controlled signaling pathways are frequently altered in human prostate cancers, making them promising targets for therapeutic strategies (DeMarzo et al., 2003; Sellers and Sawyers, 2002; Vivanco and Sawyers, 2002). The major function of the tumor suppressor *PTEN* relies on its phosphatase activity and subsequent antagonism of the PI3K/AKT pathway (Cantley and Neel, 1999; Di Cristofano and Pandolfi, 2000; Maehama et al., 2001). Loss of *PTEN* function, either in murine embryonic stem cells or in human cancer cell lines, results in accumulation of PIP3 and activation of its downstream effectors, such as AKT/PKB (Stambolic et al., 1998; Sun et al., 1999; Wu et al., 1998). As a serine/threonine protein kinase, AKT functions by phosphorylating key intermediate signaling molecules, such as

SIGNIFICANCE

Cancer of the prostate is the most common malignancy in men. Study of the biology of prostate cancer and the development of new therapies have been hampered by a lack of appropriate animal models designed to mimic genetic alterations that are frequently found in human prostate cancer. The *Pten* conditional knockout mice characterized in this study fulfilled this demand. Since the initiating oncogenic event is androgen independent, the *Pten* conditional deletion mice may provide a unique opportunity to address the mechanisms of resistance to androgen ablation therapy. By identifying possible downstream targets of PTEN-controlled prostate tumorigenesis, our findings suggest that studying genetically defined mouse models can yield valuable molecular insights that impact on human cancer research.

glycogen synthase kinase-3 (GSK3), BAD, Caspase 9, and IκB, leading to increased cell metabolism, cell growth, and cell survival (Di Cristofano and Pandolfi, 2000; Hanahan and Weinberg, 2000; Vivanco and Sawyers, 2002). Recent studies also suggest that *PTEN* may function through AKT-independent mechanisms (Freeman et al., 2003; Gao et al., 2000; Weng et al., 2001).

Inactivation of *Pten* in mouse models has confirmed *PTEN* as a bona fide tumor suppressor. *Pten*$^{+/-}$ mice showed a broad spectrum of spontaneous tumor development, with a bias toward organs such as large and small intestines, lymphoid, mammary, thyroid, endometrial, and adrenal glands (Di Cristofano et al., 1998; Podsypanina et al., 1999; Stambolic et al., 2000; Suzuki et al., 1998a). Since homozygous deletion of *Pten* causes early embryonic lethality, previous studies for prostate cancers caused by *Pten* deletion were invariably using *Pten* heterozygous mice. Different rates of prostatic hyperplasia and cancer have also been reported in the above studies. Our recent study demonstrated that *Pten*$^{+/-}$ male mice on a Balb/c/129 genetic background develop lesions (PIN) with near 100% penetrance (D. Freeman et al., submitted). However, the latency for PIN formation is rather long, approximately 10 months, and these PIN lesions never progress to metastatic disease. These results raised several questions: (1) Does the rate of *Pten* LOH determine the onset of prostate cancer initiation? (2) Is *Pten* LOH required for prostate tumor progression? and (3) What genetic changes, in addition to *Pten* deletion, are necessary for prostate cancer progression and metastasis?

Mice with combined deletion of *Pten* and other tumor suppressor genes, as possible "second hits," have been generated. *Pten*$^{+/-}$*;p27*$^{-/-}$ mice develop prostate carcinoma within 3 months postnatally with complete penetrance (Di Cristofano et al., 2001). *Pten*$^{+/-}$*;Nkx3.1*$^{-/-}$ compound mutant mice display an increased incidence of high-grade PIN but not prostate cancer (Kim et al., 2002). Similarly, Ink4a/Arf deficiency reduced tumor-free survival and shortened the latency of PIN associated with *Pten* heterozygosity (You et al., 2002). However, no metastatic prostate cancers were reported in these models (Di Cristofano et al., 2001; Kim et al., 2002; You et al., 2002). *Pten* heterozygous mice were also crossed with the well-characterized TRAMP model (Greenberg et al., 1995). *Pten* LOH significantly shortened the average life span of TRAMP mice from 245 days to 159 days (Kwabi-Addo et al., 2001). More recently, the MPAKT model was created that expressed constitutively activated AKT in mouse prostate epithelial cells (Majumder et al., 2003). The MPAKT mice develop PIN lesions in the ventral prostate with prominent bladder obstruction. No progression to metastatic prostate cancer was reported (Majumder et al., 2003).

To assess whether *Pten* homozygous deletion is critical for prostate cancer progression, we generated *Pten*$^{loxp/loxp}$*;PB-Cre4* mice to achieve prostate-specific *Pten* deletion. Our studies demonstrated that *Pten* LOH leads to a significant shortened latency of PIN formation and results in prostate cancer progression to a metastatic stage, mimicking the disease progression seen in humans. The *Pten* conditional prostate deletion mice also provide a unique opportunity to address the mechanism of resistance to androgen ablation therapy in a genetically defined model where the initiating oncogenic event is not androgen dependent. Our characterization of the *Pten* model by expression profiling has further indicated that the *Pten* model has many additional similarities to human prostate cancers.

Results

Cre-mediated *Pten* homozygous deletion and upregulated AKT activity

To achieve *Pten* prostate-specific deletion, we crossed *Pten*$^{loxp/loxp}$ mice (Lesche et al., 2002) to the *ARR2Probasin-Cre* transgenic line, PB-Cre4, in which the Cre recombinase is under the control of a modified rat prostate-specific probasin (PB) promoter (Wu et al., 2001). By crossing PB-Cre4 to a conditional reporter mouse R26R, the original report indicated that Cre expression is specific for prostatic epithelial cells. However, its expression levels vary from lobe to lobe: highest in the lateral lobe (LP), followed by the ventral (VP), dorsal (DP), and least in anterior lobes (AP) (Wu et al., 2001). Since Cre-mediated recombination event is a unidirectional process, cells with Cre-mediated gene deletion are likely to increase and accumulate over time. Indeed, a recent follow up study indicated that Cre-mediated recombination events increased to near 100% in LP/VP/DP at the age of 8 months (Powell et al., 2003).

To confirm prostate-specific *Pten* deletion, the urogenital organs as well as other tissues from *Pten*$^{loxp/+}$*;Cre*$^{+}$ mice at the age of 9 and 25 weeks were carefully dissected, and the status of *Pten* deletion was examined by sensitive PCR and immunohistochemistry (IHC) analyses. PCR analysis of 9-week-old *Pten*$^{loxp/+}$*;PB-Cre4*$^{+}$ mice showed that *Pten* deletion, as indicated by excision of the exon 5 of *Pten* gene (*Pten*$^{\Delta 5}$), is specific to the prostate gland. Except trace amount of *Pten* exon 5 deletion in the seminal vesicle, all the other tissues tested showed no detectable recombination activity (Figure 1A), consistent with the previous report (Wu et al., 2001). Double immunofluorescent analysis demonstrated that PTEN is highly expressed in cytoplasm and less so in the nucleus of prostatic epithelial cells lining the prostatic acini as well as the stromal cells surrounding the acini (Figure 1B, left panel; PTEN in red). Deletion efficiencies of the *Pten* floxed alleles in different lobes were similar to the Cre expression pattern reported previously: PTEN immunostaining is significantly reduced in the lateral and ventral lobes but only lost or diminished in a subset of the cells in the dorsal and anterior lobes of 4-week-old *Pten*$^{loxp/loxp}$*;PB-Cre4*$^{+}$ mice (Supplemental Figure S1 at http://www.cancercell.org/cgi/content/full/4/3/209/DC1, LP from WT and mutant mice are shown here). By 9 weeks, a majority of the cells in the epithelial compartment of DLP and VP show loss of PTEN immunostaining, and approximately 40%–60% cells in the AP are PTEN null (Figure 1B, right panels; PTEN in red). Furthermore, PTEN immunostaining in the stromal compartment remains positive, further confirming *Pten* epithelial-specific deletion.

As a result of PTEN loss, the AKT serine/threonine kinase, one of the primary targets of the PTEN-controlled signaling pathway, is activated. Thus, AKT phosphorylation and plasma membrane localization can serve as reliable indicators for PTEN loss. AKT phosphorylation is rarely detectable in the WT prostate (Figure 1B, left panels; P-AKT in green; also see Supplemental Figure S1B on *Cancer Cell* website) but is highly expressed in *Pten* null cells, especially at the plasma membrane of the DLP and VP (Figure 1B, right panels; also see Supplemental Figure S1F). *Pten* null, AKT-activated cells were also larger than their WT or heterozygous control cells (Supplemental Figure S1, inserts), consistent with the role of PTEN in controlling cell size (Backman et al., 2002; Groszer et al., 2001).

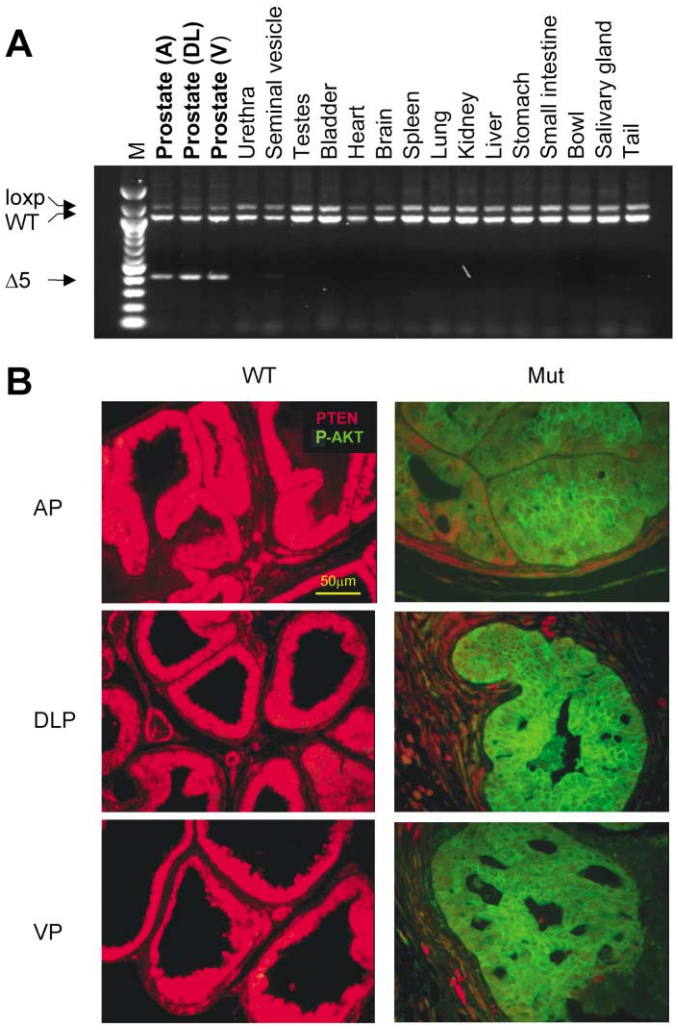

Figure 1. Conditional deletion of *Pten* tumor suppressor gene in the prostate epithelium

A: Prostate-specific *Pten* deletion. Genomic DNAs were prepared from individual prostate lobe and indicated tissues of a 9-week-old $Pten^{loxp/+}$;*PB-Cre4*$^{+}$ male mouse. PCR analysis shows *Pten* deletion (Δ5) is very prostate specific: except some leakage in the seminal vesicle, no *Pten* deletion can be detected in tissues other than the prostate.

B: *Pten* deletion correlates with AKT activation. Double immunofluorescent analysis shows the efficiencies of *Pten* deletion varies from lobe to lobe at 9 weeks postnatally. PTEN immunostaining (in red) can be detected in both nuclear and cytoplasmic compartments in the WT prostate (WT, left panels) but is almost completely lost (DLP and VP) or diminished (AP) in the *Pten* conditional mutant (Mut, right panels). In contrast, phosphor-AKT (P-AKT, in green) can be easily detected in *Pten* null but not *Pten* WT cells. Note most of stroma cells in the mutant prostate remain PTEN positive, further confirming prostate epithelium-specific deletion. AP, anterior prostate; DLP, dorsolateral prostate; VP, ventral prostate.

Pten homozygous deletion shortens latency for mPIN formation

To determine whether deletion of both alleles at the *Pten* locus, or loss of heterozygosity (LOH), is required for prostate cancer initiation and progression, we examined cohorts of littermates, WT ($Pten^{loxp/loxp}$;*PB-Cre4*$^{-}$), heterozygous ($Pten^{loxp/+}$;*PB-Cre4*$^{+}$), and homozygous ($Pten^{loxp/loxp}$;*PB-Cre4*$^{+}$) for *Pten* prostate-specific deletion from 4 to 29 weeks. To avoid potential variations contributed by genetic background, only mice from the F2 generation were used for studies described below.

Deletion of both alleles of *Pten* led to progressively enlarged prostate glands. Histological analysis indicated that from 4 weeks on, the prostates of the mutant mice developed multifocal hyperplasia. These were initially observed in the dorsolateral and ventral lobes and subsequently involved the anterior lobes as well, consistent with the efficiency of Cre-mediated *Pten* deletion. Figure 2A shows a comparison of dorsolateral lobes from WT and their *Pten* null littermates from 4 to 12 weeks. Epithelial hyperplasia, characterized by increased number of cells (without cellular atypia), is seen by 4 weeks of age (Figure 2A, a compared to b). By 6 weeks of age, these mice develop murine PIN (mPIN). mPIN is the proliferation of atypical epithelial cells within pre-existing prostatic ductules and acini (Figure 2Ad and supplemental Figure S2A on *Cancer Cell* website). This proliferation results in stratification of the epithelial layer, giving rise to distinctive architectural features, to include cribiform, tufting, or micropapillary growth patterns (Figure 2Ad). Cytological atypia is characterized by nuclear enlargement, nuclear contour irregularity, hyperchromatism, and prominent nucleoli accompanied by the inversion of the nuclear to cytoplasmic ratio (Figure 2Ac compared to 2Ad; arrows point to atypical cells). One hundred percent of the homozygous mice developed mPIN at 6 weeks (Table 1). Thus, homozygous *Pten* deletion significantly shortened the latency for mPIN formation from 8–10 months in heterozygous to 1.5 months in homozygous conditional knockouts. Significantly, *Pten* null mPIN lesions progress to invasive and metastatic cancers (see below). These results demonstrate that (1) homozygous PTEN loss alone is sufficient for prostate cancer initiation; and (2) *Pten* LOH is a rate-limiting step for prostate cancer initiation and progression.

Homozygous *Pten* deletion leads to invasive adenocarcinoma

While mice with heterozygous *Pten* deletion develop mPIN late in their lives (12–16 months, D. Freeman et al., submitted), mice with homozygous *Pten* deletion develop invasive adenocarcinoma by 9 weeks of age. Adenocarcinoma was seen in all lobes. Figure 2A compares dorsolateral lobes of WT and mutant prostate at 9 and 12 weeks. From 9 weeks onward, we have observed the extension of malignant cells, either as individual cells or as nests of acini. Initially extending through the basement membrane (Supplemental Figure S2, right panel) and subsequently through the fibromuscular layer, as shown by the loss of SMA immunostaining (Supplemental Figure S2, middle panel), the cancer cells then invaded the stroma (Figure 2Af). This in turn induces both an inflammatory and a desmoplastic response (Supplemental Figure S2, right panel). This desmoplastic response is characterized by focal stromal cellularity, found in association with the invasive cancer. These prostate cancer cells show increased proliferation compared to the WT controls, as indicated by their Ki67-positive staining (Figure 2B, left panels).

Prostate epithelium includes basal cells, luminal cells, and neuroendocrine cells. Transgenic mice overexpressing the oncogenic SV40 T antigen (Garabedian et al., 1998; Greenberg et al., 1995; Kasper et al., 1998; Masumori et al., 2001) develop both adenocarcinoma and neuroendocrine carcinoma. To define the origin of *Pten* null prostate cancers in the current model, we performed immunohistochemical analyses. Neuroendocrine

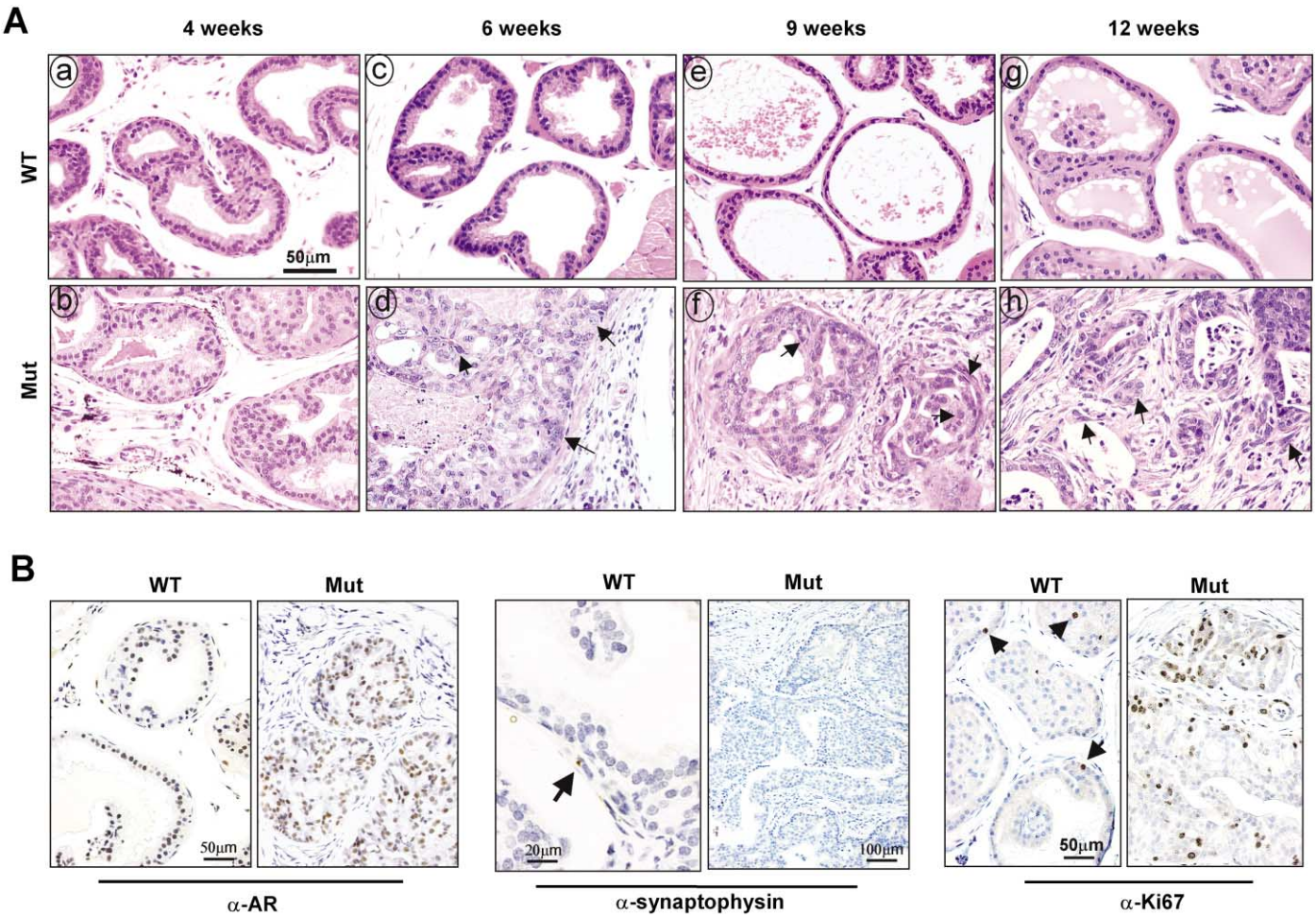

Figure 2. Homozygous *Pten* deletion leads to adenocarcinoma formation

A: A comparison of pathological phenotype of 4- to 12-week-old $Pten^{L/L};Cre^{+}$ (Mut) mice and their $Pten^{L/L};Cre^{-}$ (WT) littermate controls. Only dorsolateral lobes are shown here. Epithelial hyperplasia is seen by 4 week of age in the *Pten* null mice (a compared to b), mPIN is evident by 6 week (c compared to d; arrows point to cells with aptypia), and this progresses to invasive adenocarcinoma by 9 week of age (compare e and g to f and h).

B: Immunohistochemical analyses indicate that *Pten* null prostate cancer cells are proliferative, as indicated by Ki67-positive immunostaining (right panels), and are derived from secretory epithelium (AR+, left panels; synaptophysin-negative, middle panels). Middle left panel, high-power image shows synaptophysin-positive neuroendocrine cells in the mutant prostate (arrow).

cells in normal and neoplastic prostate are devoid of androgen receptor (AR) and are positive for chromogranin A and synaptophysin (SNP) (for review, see Sciarra et al., 2003). As shown in Figure 2B, *Pten* null cancer cells were AR positive (Figure 2B, left panels), a hallmark of secretory epithelium, but were negative for the neuroendocrine cell marker synaptophysin (Figure 2B, middle panels). Thus, *Pten* deletion results in an adenocarcinoma, i.e., epithelial origin, differing from T antigen transgenic mice in which tumors are of neuroendocrine origin.

Table 1. Phenotypes associated with *Pten* prostate-specific deletion

Age (weeks)	WT/Het	*Homozygous*
4	2/2 normal	4/4 hyperplasia
6	15/15 normal	9/9 mPIN
9–29	31/31 normal	16/16 invasive carcinoma
12–29		5/11 with metastasis
		3/14 were died

Homozygous *Pten* deletion leads to metastatic prostate cancers

Similar to the progression of human prostate cancers, *Pten* null prostate cancers also progress from mPIN to invasive adenocarcinoma, then to metastatic carcinoma with precisely defined kinetics. We have observed lymphovascular invasion in the *Pten* conditional knockout mice from 12 weeks of age (present in 5 of 11 mice, Table 1; Figures 3Aa, 3Ab, 3Ae, and 3Af) with subsequent seeding of the subcapsular sinuidal regions of draining lymph nodes (2 of 11 mice; Figures 3Ac and 3Ag; also see supplemental Figure S3) and pulmonary alveolar spaces (3 of 11 mice; Figures 3Ad and 3Ah). The metastatic tumor cells in the lung alveolar space remain AR positive (Figure 3B, left panel) and are negative for PTEN immunostaining (Figure 3B,

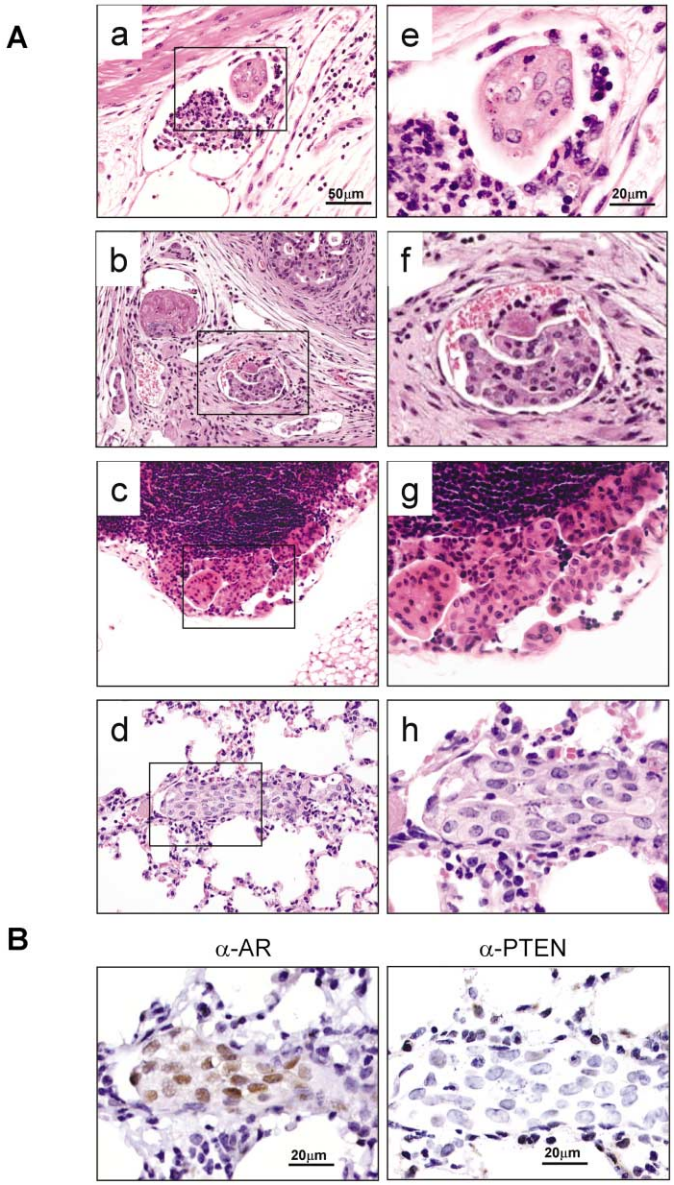

Figure 3. Homozygous *Pten* deletion leads to metastatic prostate cancer

A: H&E stained sections show metastatic prostate cancer cells in the lymphovascular system (a and b), subcapsular sinus of a lymph node (c), and alveolar spaces of the lung (d). A higher magnified picture (boxed region) is shown on the right.

B: Immunohistochemical analyses show that metastatic cells in the pulmonary alvelolar spaces are AR positive (left) and PTEN negative (right).

right panel). Thus, the conditional *Pten* null mouse represents the first animal model in which deletion of an endogenous gene leads to metastatic prostate cancer.

Pten null prostate tumors do respond to castration

Androgens are critical both for development and function of the normal prostate gland and for the survival and proliferation of prostate cancer cells. To assess the response of *Pten* null prostate cancers to hormone ablation therapy, we castrated *Pten* conditional knockout mice at 16 weeks, when invasive adenocarcinoma has already formed, and analyzed the immediate response of *Pten* null tumors at 3 and 6 days post-castration. In response to androgen withdrawal, the AR-positive prostatic epithelium undergoes increased apoptosis, as indicated by dramatically increased TUNEL-positive cells, which results in a reduction of prostate volume following castration (Supplemental Figures S4 and S5 on *Cancer Cell* website). In the WT control prostate, cell death can be easily detected 3 days after castration and peaks around 6 days (Figure 4A, TUNEL+ cells in brown; blue bars on the right panel show quantification). Even though *PTEN* is known for its role in negatively regulating apoptosis (Di Cristofano et al., 1998), quantitative analysis indicates that there is almost 10 times increase of apoptotic cells in the *Pten* null prostate 3 days post-castration compared with intact animal (Figure 4A, red bars; $p < 0.005$), suggesting that the survival of *Pten* null prostate cancer cells is androgen dependent. The percentage of apoptotic cell drops when the measurement is taken at 6 days post-castration (Figure 4A, $p < 0.005$), indicating that *Pten* null prostate cancer cells may adapt to the new condition and exhibit enhanced survival, or the androgen-sensitive population has been gradually depleted.

To test whether mice with *Pten* null prostate cancer would benefit from androgen ablation therapy, we castrated *Pten* conditional knockouts at 2.5–4 months when invasive adenocarcinoma has already formed. For intact mice, 3/14 *Pten* prostate conditional knockouts died by the age of 12–29 weeks (Table 1). In contrast, no lethality is observed in 8/8 castrated *Pten* null mice aged from 7–10 months, indicating that *Pten* null prostate cancers do benefit from androgen ablation therapy. However, when these mice were sacrificed 2.5 months after castration, we found that a substantial number of *Pten* null prostate cancer cells remained (Figure 5). Histological analysis demonstrates that *Pten* null prostate glands remain 5- to 10-fold larger when compared to age-matched WT controls (Figure 5, left panels; comparing LP of WT and mutant). Residual invasive adenocarcinoma is clearly evident (Figure 5, lower middle panel; red arrows point to cords of cancerous cells coursing through desmoplastic stroma). This enlargement, at least in part, is due to the higher proliferation index in the *Pten* null prostate. Figure 4B shows Ki67 staining and quantification (Figure 4B). Surprisingly, the proliferation indexes of *Pten* null prostate are 17-fold higher than age- and genetic background-matched WT controls at 3 days, as well as 6 days and 10 weeks, after castration and are comparable to the pre-castration stage, suggesting that *Pten* deletion leads to androgen-independent or semi-independent cell proliferation. Interestingly, while most of the *Pten* null prostate cancer cells remain AR positive, it exhibits a more diffuse, heterogeneous immunostaining pattern (Figure 5, right panels). The *Pten* null prostate cancer cells are likely to be sensitive to androgen, as indicated by the higher percentage of TUNEL-positive cells found in *Pten* null prostate 10 weeks after castration (Figure 4A). Even though the remaining adenocarcinoma in *Pten* conditional knockouts did not lead to premature death during the short observation period, the knockouts may have the potential, as indicated by their ability to proliferate in the absence of androgen, to develop into HRPC, similar to that of humans, after prolonged castration.

Gene expression analysis revealed similarities between molecular mechanisms underlying *Pten* null murine cancers and human prostate cancers

To provide insights into the molecular events associated with prostate tumorigenesis, we compared gene-expression profiles

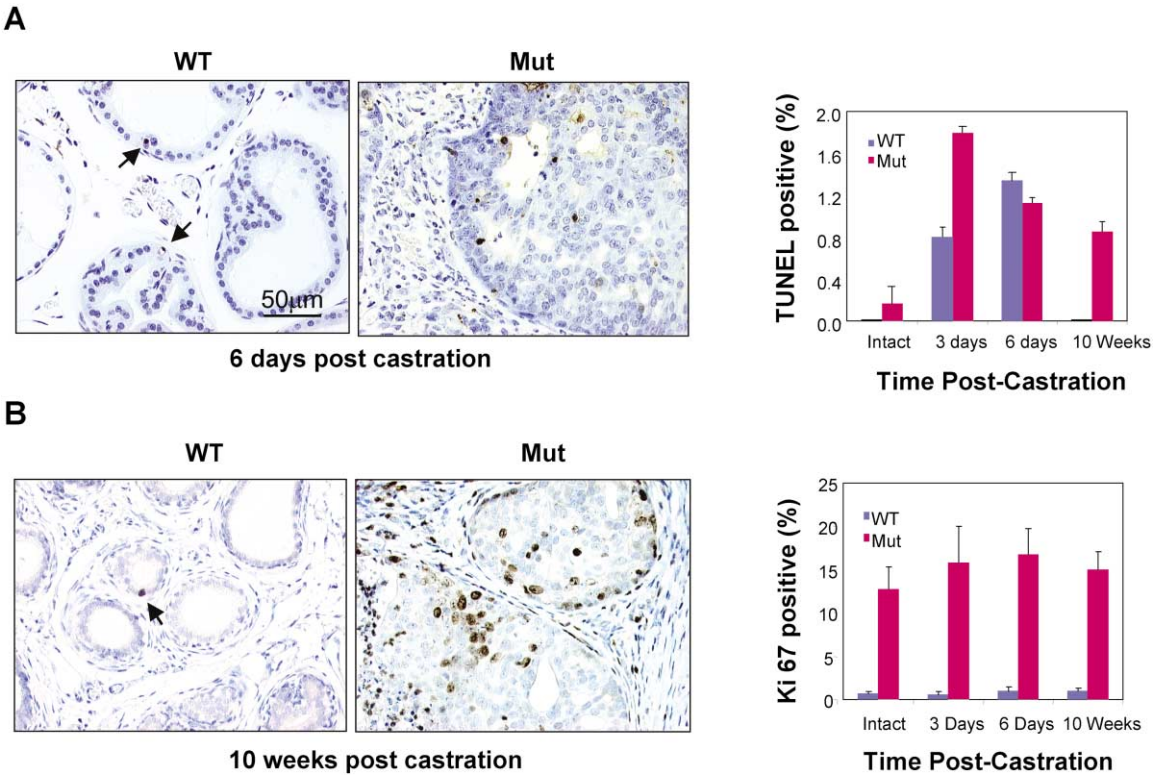

Figure 4. *Pten* null prostate cancers in response to androgen ablation therapy

A: TUNEL assay. 16-week-old *Pten* conditional knockouts (Mut) and their WT littermates were castrated for indicated period, and prostate tissues were harvested for TUNEL analysis. Left, TUNEL-positive cells are present in WT and Mut prostates 6 days post-castration; right, quantification. 16-week-old noncastrated males (intact) were used as controls. $p < 0.005$.

B: *Pten* null prostate cancer cells remain proliferative in the absence of androgen. Tissue sections from the aforementioned animals were stained with anti-Ki67 antibody, an indicator of proliferating cells. Left, Ki67-positive cells are present in the prostate glands 10 weeks post-castration; right, quantification. $p < 0.005$.

of *Pten* null prostates with age-matched WT controls using microarray analysis. Our initial studies were focused on animals 26–29 weeks of age since 100% of mutant animals at this stage have already developed invasive adenocarcinoma. Half of the prostate was fast frozen for RNA preparation and the other half was fixed for pathological evaluation. Histological analysis indicated that more than 80% of the *Pten* null prostate tissue at this stage was composed by microinvasive cancer cells and mPIN and less than 20 percent by stoma and inflammatory cells (data not shown). Statistical analysis of 10290 mouse genes/ESTs generated a list of 1041 significantly altered genes/ESTs (Table S1 in Supplemental Data). Among them, 579 are upregulated in *Pten* null cancer and 462 are downregulated, and the top 50 up- and downregulated genes are shown in Figure 6A.

Gene expression changes in the *Pten* null prostate cancers included orthologs of genes whose expression also changes in human prostate cancers, such as upregulated cyclin A, clusterin, PSCA, S100P, ERG-1, and osteopontin, as well as down regulated Nkx3.1 and myosin heavy chain 11 (Aaltomaa et al., 1999; Bowen et al., 2000; Dhanasekaran et al., 2001; Gu et al., 2000; He et al., 1997; Hotte et al., 2002; Mousses et al., 2002; Ramaswamy et al., 2003; Reiter et al., 1998; Steinberg et al., 1997). The corresponding protein expression levels of selected genes, which are underlined in Figure 6A, were further confirmed by immunohistological staining or Western blot analysis. As shown in Figures 6B and 6C and summarized in Figure 7, some changes, such as Nkx3.1 and clusterin (also see Supplemental Figure S1), are directly associated with homozygous *Pten* deletion and may be regulated by a PTEN-controlled signaling pathway; other changes are observed during tumor progression, such as PSCA (Figure 6B), or related to metastasis (osteopontin, Z. Song and P.R.-B., personal communication). These later groups may represent the additional genetic alterations associated with prostate cancer development (Figure 7). Clusterin (Steinberg et al., 1997) and osterpontin (Hotte et al., 2002) are secreted molecules and could be used as potential biomarkers for cancer staging and molecular diagnostics.

Recently, molecular signatures of metastatic potential have been found within the bulk cell mass of primary tumors, suggesting that metastasis may be an intrinsic property inherited in the primary cancers (Ramaswamy et al., 2003; van 't Veer et al., 2002). Interestingly, among 17 such "signature genes" identified in various human cancers, three genes, namely Col1α1, Col1α2, and Myh11, are also up- or downregulated in our *Pten* prostate models (Figure 6A, genes are marked with *), consistent with the metastasis potential of *Pten* prostate cancer cells described in this study. Taken together, our initial characterization of changes in gene expression profiling suggests that the *Pten* prostate model will be useful to provide insights into the molecular events associated with prostate cancer progres-

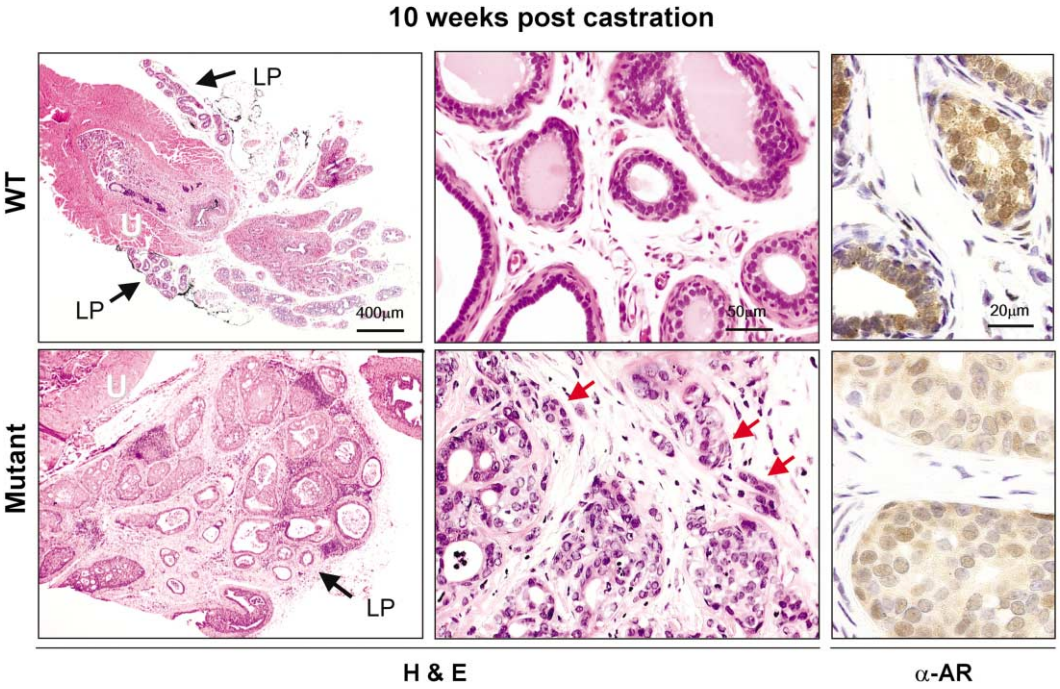

Figure 5. Invasive adenocarcinoma remains in the *Pten* null prostate 2.5 months post-castration

Left panels, H&E stained section show enlarged prostate gland in *Pten* conditional knockout, as compared to its WT littermate after 2.5 months of castration. Arrows indicate lateral prostate lobes (all images taken at the same magnification). Middle panels, invasive adenocarcinoma in *Pten* conditional knockout. Note cords of cancerous cells (red arrows) are mixed with reactive stroma. Right panels, AR-positive staining in WT and mutant prostate tissues 10 weeks post-castration. Note AR immunostaining is weaker and more heterogeneously diffused post-castration.

sion and metastasis and to elucidate biomarkers and drug targets for clinical classification and therapeutic intervention.

Discussion

Animal models for human prostate cancer

Animal models that mimic genetic alterations and clinical courses of human prostate cancer are at high demand for the study of the molecular mechanisms underlying prostate tumorgenesis and for innovation and validation of new anti-cancer strategies. Currently available models for prostate cancer research include Huggins' spontaneous canine model, the Dunning and Noble rat models, the prostate organ reconstitute model, and several transgenic mouse models (Powell et al., 2003). Mouse models, created via either transgenic or knockout approaches, are more frequently utilized than the canine or rat models because of their clearly defined genetics and molecular targets. So far, the transgenic adenocarcinoma mouse prostate (TRAMP) is the only mouse prostate cancer model that progresses beyond the PIN lesion. However, this SV40 T antigen transgenic model has high neuroendocrine differentiation potential (Garabedian et al., 1998), a phenotype morphologically and biologically distinct from the adenocarcinomas seen in most human prostate cancers (Powell et al., 2003). The SV40 T antigen model also has the limitation that the oncogene is driven by an androgen-dependent promoter and, therefore, it is not an ideal model for studying the mechanism of androgen independence after androgen ablation. The attempt of genetic inactivation of several classic tumor suppressor genes, such as *Rb1, Tp53,* and *Cdkn1B,* has yielded little information regarding their involvement in prostate cancer development. Mice lacking *Rb1* are embryonic lethal, and *Tp53, Cdkn1B* (*p27KIP1*), or *Nkx3.1* deletion either has no effect on prostate cancer development (*Tp53* and *Cdkn1B*) (Powell et al., 2003) or results in only a hyperplasia/dysplasia phenotype in aged animals (*Nkx3.1*) (Abdulkadir et al., 2002; Bhatia-Gaur et al., 1999; Tanaka et al., 2000).

As summarized in Figure 7, the *Pten* prostate cancer model mimics the course of human prostate cancer formation: it progresses from hyperplasia to mPIN, then to invasive adenocarcinoma, followed by matastasis. Histologically, the *Pten* null tumor is derived from secretive epithelium, similar to the origin of the majority of human prostate tumors. Notably, the invasive *Pten* null prostate cancer cells do respond to androgen ablation, as indicated by increased apoptosis, similar to most human prostate cancers. Even though the survival of *Pten* null prostate cancer cells is androgen sensitive, their proliferation is not affected by androgen withdrawal. The property of androgen-independent growth observed in *Pten* null prostate cancers may contribute to hormone-resistant prostate cancer formation. Finally, *Pten* homozygous deletion leads to gene expression changes seen in human prostate cancers and shares similarities with other human cancers with metastatic potentials. Thus, *Pten* prostate conditional knockout mice described in this study may serve as a very useful tool for studying the molecular mechanisms underlying prostate cancer metastasis and HRPC formation.

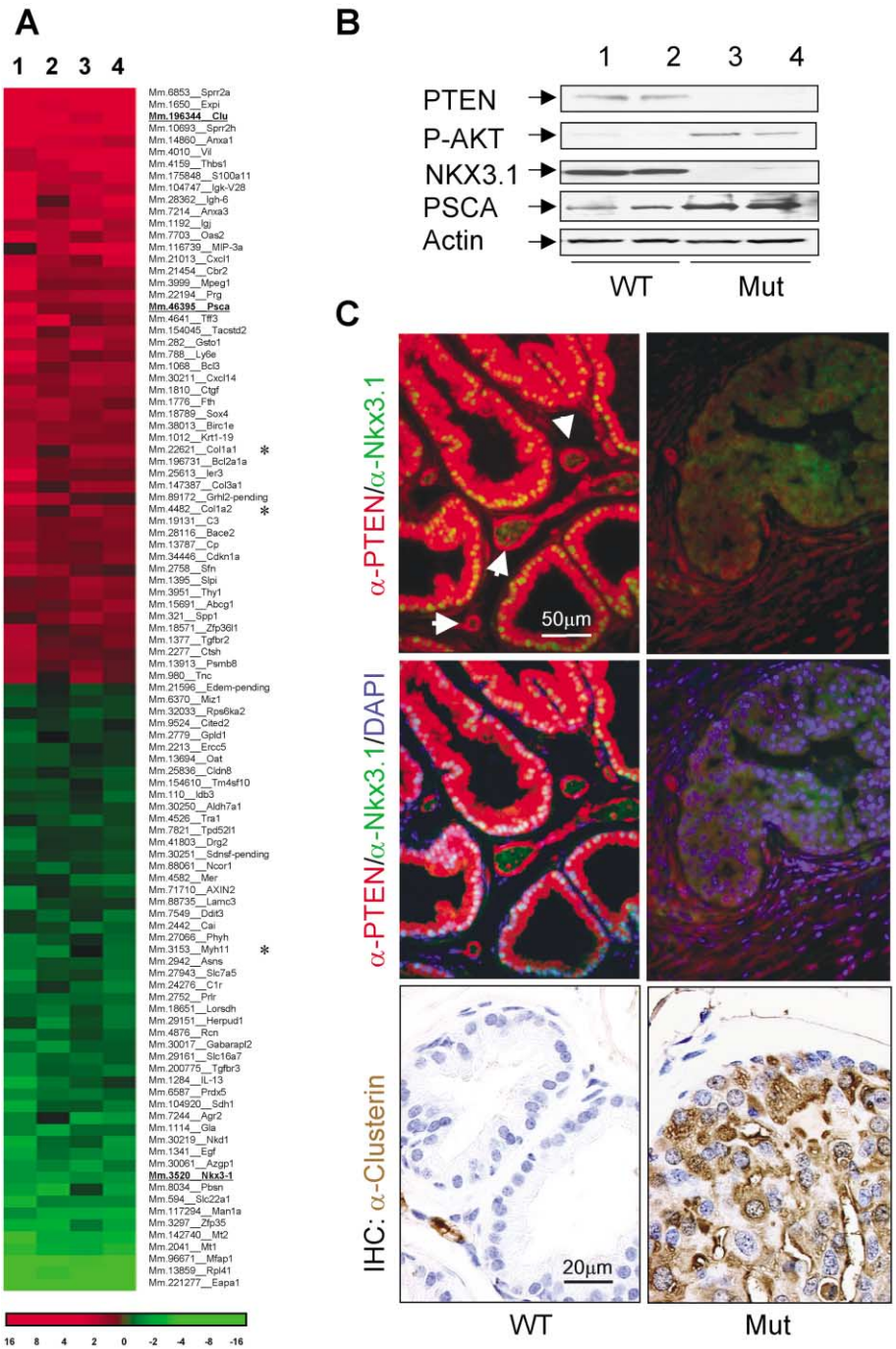

Figure 6. *Pten* deletion leads to dysregulated gene expressions recapturing molecular changes seen in human disease

A: A list of top 100 dysregulated genes. RNAs extracted from four pairs of WT and Mut littermates were used for microarray analysis. Genes with significantly altered expression were identified by SAM analysis. Heat map colors reflect fold-change values of the ratio in each pair. Genes whose expression changes are further confirmed by either Western blot or immunohistochemistry are underlined. Signature genes associated with human cancer metastasis are marked with "*."

B: Western blot analysis. Loss of PTEN leads to increased AKT phosphorylation, decreased NKX3.1 protein level, and increased PSCA expression in *Pten* null mice.

C: Altered NKX3.1 and Clusterin expressions in 9-week-old *Pten* null prostate. Upper panels, double immunofluorescent staining for PTEN (in red) and Nkx3.1 (in green) indicates that PTEN and NKX3.1 are colocalized in the nucleus of WT prostatic epithelium (in yellow). Such localization is lost in the mutant prostate (right). Note no colocalization can be detected in the blood vessels (white arrows) where NKX3.1 is not expressed. Middle panels show above sections with DAPI staining to localize the nucleus. Lower panels, Immunohistochemical analysis for increased clusterin expression in the mutant prostate.

Prostate cancer metastasis

Prostate cancers are known to metastasize; however, so far very little is known regarding the mechanisms governing prostate cancer metastasis (Cher, 2001; Mundy, 2002). The process of metastasis is often regarded as a multistep event, and each event must be successful for the entire process to occur. The successful metastatic cell must leave the primary site, enter and survive in the lymphatic and blood circulatory systems, overcome host defenses, extravasate and grow as a metastatic colony (Fidler and Kripke, 2003). Thus it is believed that the metastatic cell is a rare cell mixed within the heterogenous tumor population. This notion is primarily supported by animal models in which poorly metastatic cell lines can spawn highly metastatic variants after multiple rounds of selection (Clark et al., 2000; Fidler and Kripke, 1977). Recently, molecular signatures of metastatic potential are found within the bulk of primary tumors (Ramaswamy et al., 2003; van 't Veer et al., 2002), suggesting that metastasis may be an intrinsic property inherited in the primary cancers.

Interestingly, the expressions of 3 out of 17 such signature genes were altered in the same directions in our model, indicating that the *Pten* conditional knockout mice may provide a

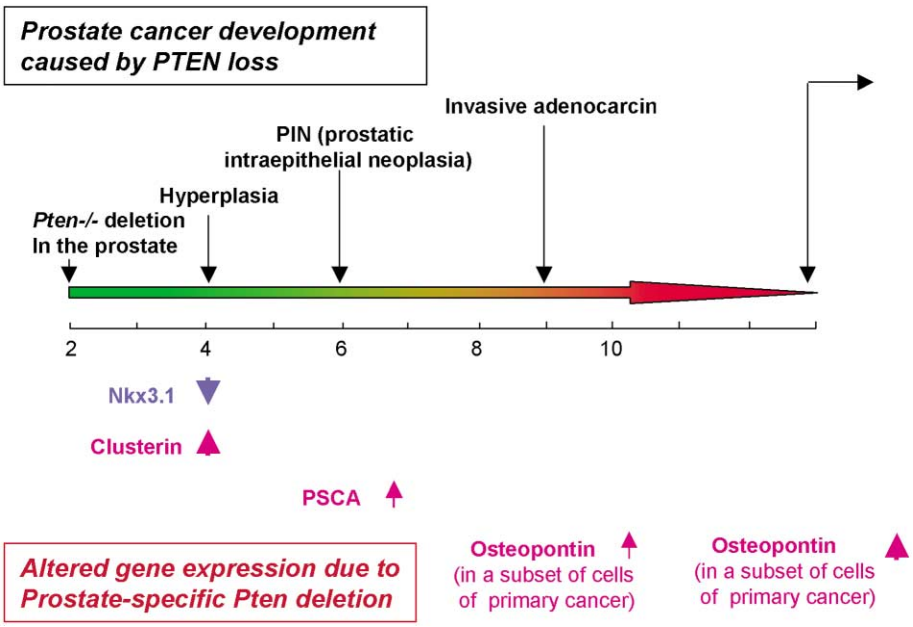

Figure 7. A summary of the onset and progression of prostate cancer development in mice with homozygous *Pten* deletion in the murine prostate epithelium and changes in gene expression

unique tool to study the molecular mechanisms underlying prostate cancer metastasis. In fact, among 11 *Pten* conditional knockout mice age 12–29 weeks, 5 had lymphovascular invasion by the prostatic cancer cells. Distance metastases lesions were found in the lymph nodes and lung. Even though autopsy survey indicates possible metastatic foci in other organs, most of the metastasis lesions are very small and can be easily missed during histology sectioning. Thus, the actual rate of metastasis could be higher than what we have identified pathologically.

A unique property of prostate cancer is the frequently observed bone metastasis and subsequent osteoblastic/osteoclastic lesions (Bubendorf et al., 2000; Cher, 2001; Harada et al., 1992; Mundy, 2002). Even though we have not positively identified colonies of prostate cancer cells in bone metastases, we did observe dramatic bone remodeling activity in 3/11 aged $Pten^{loxp/loxp};Cre^{+}$ mice (data not shown). Our analyses also detected increased osteopontin expression levels (Supplemental Table S1, and Z. Song, personal communication), an event known to associate with the presence of bone metastasis in men with prostate cancer (Hotte et al., 2002; Thalmann et al., 1999). Further studies using sensitive imaging methodologies and more prostate-specific markers will help to address this issue.

Changes in gene expression profiling

From the top 100 most significantly regulated genes of our cDNA array analysis, we identified several genes that were well documented in the literature for participating prostate cancer initiation, progression, and metastasis.

One of the most interesting genes is *Nkx3.1*. *Nkx3.1* is located in human chromosome 8p21, a region frequently deleted in human prostate cancer (He et al., 1997), and its inactivation has been shown to correlate with prostate cancer initiation and progression (Bowen et al., 2000). Interestingly, the mechanism of Nkx3.1 loss in *Pten* null prostate cancers may differ from the Myc transgenic model (Ellwood-Yen et al., 2003 [this issue of *Cancer Cell*]). Instead of gradual and cancer stage-dependent Nkx3.1 downregulation observed in the Myc model, we found that Nkx3.1 loss is directly correlated with PTEN loss and AKT activation. This correlation can be observed as earlier as 4 weeks, a pre-cancer stage (Supplemental Figure S1). Interestingly, some of the genes known to be regulated by NKX3.1(Magee et al., 2003), such as probasin, are also downregulated in *Pten* null prostate cancers (Figure 6A). This result suggests that the mechanisms of Nkx3.1 loss of function in human prostate cancers may depend on the initial tumorgenic events. Indeed, synergistic effect of PTEN and NKX3.1 on tumor initiation has been reported (Kim et al., 2002).

PSCA is another molecule that we identified by microarray and confirmed to be upregulated in *Pten* null prostate cancer. PSCA is expressed in almost all cases of high-grade PIN and is overexpressed in 40% of local and as many as 100% of bone metastatic prostate cancers (Gu et al., 2000). Our array analysis demonstrated that the expression of PSCA is upregulated by 14-fold in *Pten* null adenocarcinoma, consistent with our previous report that the percentage and intensity of mPSCA-positive cells increases dramatically in *Pten* mutant prostates (Dubey et al., 2001). However, further experiments are necessary to distinguish whether PSCA serves as a marker for a unique subpopulation of prostate epithelial cells associated with PTEN-controlled cell transformation or acts as an important player in the process of prostate cancer formation caused by *Pten* loss.

Another robust upregulated gene is clusterin. Clusterin, also known as testosterone-repressed prostate message-2 (TRPM-2), dimeric acid glycoprotein, and sulfated glycoprotein-2 (SGP-2), is a highly conserved glycoprotein cloned from regressing rat ventral prostate tissue. Recent studies implicated a protective function of clusterin against apoptosis in several tissues (July et al., 2002). Clusterin may also be involved in the development of androgen independence and resistance to chemotherapy (July et al., 2002; Steinberg et al., 1997). The early onset and persistence of clusterin overexpression indicates clusterin may contribute to cancer initiation and progression in our model.

***Pten* prostate cancer model and androgen ablation therapy**

The seminal works conducted more than 60 years ago by Huggins (Huggins et al., 1941) have addressed some of the most fundamental questions regarding the requirement of androgen for normal prostate cell as well as prostate cancer cell growth and survival (Denmeade and Isaacs, 2002). However, the molecular basis underlying the development of androgen-independent prostate cancer growth after androgen ablation therapy, or HRPC, has not been resolved to date.

What is the cellular origin of HRPC? The normal prostatic epithelium consists of at least three cell types, basal cells, secretory luminal cells, and neuroendocrine cells (Bui and Reiter, 1998; Isaacs, 1999). The secretory luminal cells are terminally differentiated and androgen dependent and will undergo atrophy and die upon androgen withdrawal. Neuroendocrine cells do not express androgen receptor (AR) and thus are androgen independent. Basal cells are generally considered to be androgen independent, although their progeny, the intermediate precursors, do express low levels of AR and are potentially androgen responsive. Therefore, HRPC could derive from (1) a subpopulation of androgen-independent tumor cells that is present before hormone ablation therapy (Isaacs, 1999) or (2) cells that gained androgen independency due to additional genetic alterations and selected out after castration (Craft et al., 1999). The *Pten* prostate cancer cells are AR positive and do respond to androgen ablation therapy. However, the *Pten* null cells remain proliferative after prolonged castration (Figure 4B). Thus, *Pten* deletion either renders prostate cancer cells to proliferate in the absence of androgen and/or mobilizes androgen-independent basal cells to enter cell cycle. Further studies, such as colocalizing Ki-67-positive cells with different prostatic cell-specific markers, will help in distinguishing these possibilities.

On the molecular level, it has been proposed that restoration of AR activity is critical for androgen-refractory prostate cancer cells, based on clinical findings that HRPC still expresses AR and androgen-regulated genes, such as prostate-specific antigen (PSA). Several recent studies suggest the presence of crosstalks between the PI 3-kinase/Akt and AR signaling pathways. Unfortunately, the effects in different cell lines and from different labs often seem contradictory, leading to confusion in the field as to whether PI3K/Akt exerts a positive or negative effect on AR. For example, Manin et al. have claimed that the PI 3-kinase/Akt pathway is required for basal and dihydrotestosterone-induced AR expression in prostate cell lines (Manin et al., 2002); whereas Lin et al. have shown that AKT and Mdm2 form a complex with AR and promote phosphorylation-dependent AR ubiquitination, resulting in AR degradation by the proteasome (Lin et al., 2002). It is clear from our study that activation of PI3-kinase/AKT signaling pathway cannot prevent cell death caused by androgen ablation. Thus, if there is a crosstalk between AR and PI3-kinase/AKT pathways in vivo, the effects will not be significant in preventing androgen-sensitive cells from apoptosis. Consistent with this notion, a recent study suggested that FKHR/AR complex may play an important role in protection of prostate cancer cells from apoptosis through AKT-independent pathway (Li et al., 2003). Whether AKT activation will lead to androgen-independent cell proliferation, either mediated by AR or independent of AR, remains to be investigated.

Experimental procedures

Generation of prostate-specific *Pten* exon 5 deletion *Pten$^{L/L}$;C^{+}* mice

To generate *Pten$^{L/L}$;C^{+}* mice, *ARR2Probasin-Cre* transgenic line, PB-Cre4 (Wu et al., 2001) on C57BL/6xDBA2 background were crossed to *Pten$^{L/L}$* mice on a 129/Balb/c background. The males offspring with *Pten$^{L/+}$;C^{+}* genotype were then crossed to *Pten$^{L/L}$* females. Only F2 generation of male offspring was used in this study.

Histology and immunochemistry analysis

Tissues are fixed in 10% buffered Formalin for 6–10 hr, followed by gentle wash and transfer to 70% alcohol. These paraffin-embedded tissues were sectioned (4 μm) and stained with hematoxylin & eosin. All IHC staining was performed on 4 μm sections that were prepared from paraffin-embedded blocks and placed on charged glass slides. Antigen retrieval was performed by incubating the slides in 0.01 M citric acid buffer (pH 6.0) at 95°C for 30 min. Slides were then allowed to cool for 20 min in citric acid buffer. After washing in deionized water, the slides were then transferred to PBS (pH 7.4) (2 × 5 min each). The endogenous peroxidase activity was inactivated in a solution containing 3% hydrogen peroxide (H_2O_2) in methanol. The following detection and visualization procedures were performed according to manufacturer's protocol. Slides were counterstained in Mayer's hematoxylin, dehydrated, cleared, and coverslipped. Negative control slides were run without primary antibody. Control slides known to be positive for each antibody were incorporated.

For AR (PG-21, Upstate Biotechnology) and Nkx3.1 (DE#2, a kind gift from Dr. Abate-Shen at the Center for Advanced Biotechnology and Medicine, Robert Wood Johnson Medical School) staining, pretreated sections were first blocked with 10% normal goat serum and then the primary antibodies were diluted as suggested by the manufacturer and incubated overnight at 4°C. Following three washes with PBS, the antigens were visualized using the biotin-streptavidin based detection system from BioGenex. For clusterin-β (M-18, Santa Cruz Biotechnology) staining, the normal goat serum blocking was omitted.

For PTEN (26H9, Cell Signaling Technology) and P-AKT (#9277, Cell Signaling Technology) staining, pretreated sections were first blocked with mouse Ig blocking reagent in the VECTOR M.O.M. Immunodetection Kit (Vector Laboratories) and then incubated with primary antibody at room temperature for 30 min.

For fluorescence double staining, the section was treated as above and first stained with mouse antibody (PTEN) followed by signal amplification with TSA Plus Fluorescence Systems (PerkinElmer). After biotin blocking, the section was then stained with rabbit antibody (NKX3.1, P-AKT), and signal was amplified with TSA system with different fluorescence.

Apoptosis and proliferation index

Cells undergoing apoptosis were determined by TUNEL assay using the In Situ Cell Death Detection Kit from Roche according to manufacturer's instruction. Sections were de-waxed with xylene and rehydrated through graded alcohol. DNA fragmentation was labeled with fluorescein-conjugated dUTP and visualized with converter-POD and DAB. Apoptotic cell was identified by positive TUNEL staining and the appearance of apoptotic body. Five hundred cells were counted from five different view fields, and the TUNEL-positive cells were presented as numbers per 100 nucleated cells. Cell proliferation index was determined by Ki67 staining and calculated as above except 100 nucleated cells were counted per view field.

Microarray preparation

Custom cDNA microarrays enhanced for genes expressed in the mouse prostate were prepared on poly-lysine-coated glass microscope slides using a robotic spotting tool as previously described (Aaltomaa et al., 1999). Each array consisted of 10290 unique mouse cDNAs, 4511 of which were derived from cDNA libraries of developing and mature mouse prostate (http://www.mpedb.org) (Nelson et al., 2002). The remaining 5779 cDNAs were chosen from the Research Genetics sequence-verified set of IMAGE clones (http://www.resgen.com/products/SVMcDNA.php3) and from the National Institute of Aging 15K set. The clone inserts were amplified by PCR, purified, and analyzed by gel electrophoresis. All PCR products were sequence-

verified prior to spotting. Additional control cDNAs were included, and some clones were spotted twice for a total of 11552 features on the array.

Probe construction, microarray hybridization, and data acquisition

The protocol used for indirect labeling of cDNAs was described previously (Pritchard et al., 2001). Briefly, cDNA probes that incorporate aminoallyl dUTP (aa-dUTP; Sigma-Aldrich) were made using 30 μg of total RNA. Purified cDNA from *Pten* null and age-matched wild-type prostates was labeled with either Cy3 or Cy5 monoreactive fluors (Amersham Life Sciences), combined, and competitively hybridized to microarrays under a coverslip for 16 hr at 63°C. Fluorescent array images were collected for Cy3 and Cy5 emissions using a GenePix 4000B fluorescent scanner (Axon Instruments, Foster City, California). Image intensity data were extracted and analyzed using GenePix 4.0 microarray analysis software. RNA from four *Pten* null prostates and four age-matched wild-type prostates was analyzed using the microarray. Each experiment was performed in duplicate with reversal of the fluorescent label to account for dye effects.

Data normalization and statistical analysis

Log_2-ratios of PTEN/WT signal were normalized using a print tip-specific intensity-based scatter plot smoother that uses robust locally linear fits to capture the dependence of the log-ratios on overall log-spot intensities (Dudoit, 2000). Statistical Analysis of Microarrays (SAM) software was used to determine genes that showed statistically significant differences in *Pten* null mice (Tusher et al., 2001). At a delta of 2.36, 579 genes were significantly upregulated in *Pten* null prostates and 462 were downregulated. The median false discovery rate (FDR) was 0.085%, which predicts that ~1 of the 1041 differentially expressed genes is falsely discovered. The differentially expressed genes other than ESTs were clustered and visualized with the Cluster and TreeView program from Dr. Eisen's laboratory, and the top 50 most significant were presented.

Western blot analysis

Extract was prepared by sonicating prostate tissues in buffer containing 50 mM Tris-HCl (pH 7.5), 150 mM NaCl, 0.5% NP-40, 1 mM EDTA, 1 mM PMSF, and cocktail protease inhibitors (Roche). Seventy micrograms tissue lysate were subjected to SDS-PAGE followed by Western blot analysis using anti-PTEN (9552, cell signaling), phospho-Akt (9271, cell signaling), NKX3.1 (a kind gift by Dr. Abate-Shen), PSCA (a kind gift by Dr. Owen Witte from UCLA), and actin (A 4700, sigma) antibodies, respectively.

Acknowledgments

We thank Drs. Sawyers, Chow, Wu, Herschman, and Reiter and members of our laboratories for helpful comments; Drs. Ellwood and Sawyers for exchanging unpublished results; Dr. Robert Cardiff and Robert J. Munn for pathology analysis; Dr. Abate-Shen for anti-Nkx3.1 antibody; Drs. Reiter and Witte for anti-PSCA antibody; Dr. Lily Wu for AR immunohistochemistry; and Ms. Lawson for technical assistance. H.W. is an Assistant Investigator of the Howard Hughes Medical Institute (HHMI). S.W and G.L. are supported by the grant from DOD: PC991538 and NIH CA98013. G.V.T. is supported by a grant from DOD: PC010383 and UCLA Prostate SPORE career Development grant. P.S.N. is supported in part by a Damon Runion scholar award. This work was partially supported by grants from NIH: CA98013, DOD: PC991538, and CapCure (to H.W.), and NIH CA 59705 (to P.R.-B.), and NIH DK65204 and DK59125 (to P.S.N.).

Received: April 22, 2003
Revised: July 27, 2003
Published: September 22, 2003

References

Aaltomaa, S., Eskelinen, M., and Lipponen, P. (1999). Expression of cyclin A and D proteins in prostate cancer and their relation to clinopathological variables and patient survival. Prostate *38*, 175–182.

Abdulkadir, S.A., Magee, J.A., Peters, T.J., Kallem, Z., Naughton, C.K., Humphrey, P.A., and Milbrand, J. (2002). Conditional loss of Nkx3.1 in adult mice induces prostatic intraepithelial neoplasia. Mol. Cell. Biol. *22*, 1495–1503.

Backman, S., Stambolic, V., and Mak, T. (2002). PTEN function in mammalian cell size regulation. Curr. Opin. Neurobiol. *12*, 516–522.

Bhatia-Gaur, R., Donjacour, A.A., Sciavolino, P.J., Kim, M., Desai, N., Young, P., Norton, C.R., Gridley, T., Cardiff, R.D., Cunha, G.R., Abate-Shen, C., and Shen, M.M. (1999). Roles for Nkx3.1 in prostate development and cancer. Genes Dev *13,* 966–977.

Bose, S., Crane, A., Hibshoosh, H., Mansukhani, M., Sandweis, L., and Parsons, R. (2002). Reduced expression of PTEN correlates with breast cancer progression. Hum. Pathol. *33*, 405–409.

Bowen, C., Bubendorf, L., Voeller, H.J., Slack, R., Willi, N., Sauter, G., Gasser, T.C., Koivisto, P., Lack, E.E., Kononen, J., et al. (2000). Loss of NKX3.1 expression in human prostate cancers correlates with tumor progression. Cancer Res. *60*, 6111–6115.

Bubendorf, L., Schopfer, A., Wagner, U., Sauter, G., Moch, H., Willi, N., Gasser, T.C., and Mihatsch, M.J. (2000). Metastatic patterns of prostate cancer: an autopsy study of 1,589 patients. Hum. Pathol. *31*, 578–583.

Bui, M., and Reiter, R.E. (1998). Stem cell genes in androgen-independent prostate cancer. Cancer Metastasis Rev. *17*, 391–399.

Cantley, L.C., and Neel, B.G. (1999). New insights into tumor suppression: PTEN suppresses tumor formation by restraining the phosphoinositide 3-kinase/AKT pathway. Proc. Natl. Acad. Sci. USA *96*, 4240–4245.

Cher, M.L. (2001). Mechanisms governing bone metastasis in prostate cancer. Curr. Opin. Urol. *11*, 483–488.

Clark, E.A., Golub, T.R., Lander, E.S., and Hynes, R.O. (2000). Genomic analysis of metastasis reveals an essential role for RhoC. Nature *406*, 532–535.

Craft, N., Chhor, C., Tran, C., Belldegrun, A., DeKernion, J., Witte, O.N., Said, J., Reiter, R.E., and Sawyers, C.L. (1999). Evidence for clonal outgrowth of androgen-independent prostate cancer cells from androgen-dependent tumors through a two-step process. Cancer Res. *59*, 5030–5036.

Dahia, P.L. (2000). PTEN, a unique tumor suppressor gene. Endocr. Relat. Cancer *7*, 115–129.

DeMarzo, A.M., Nelson, W.G., Isaacs, W.B., and Epstein, J.I. (2003). Pathological and molecular aspects of prostate cancer. Lancet *361*, 955–964.

Denis, L., and Murphy, G.P. (1993). Overview of phase III trials on combined androgen treatment in patients with metastatic prostate cancer. Cancer *72*, 3888–3895.

Denmeade, S.R., and Isaacs, J.T. (2002). A history of prostate cancer treatment. Nat. Rev. Cancer *2*, 389–396.

Deocampo, N.D., Huang, H., and Tindall, D.J. (2003). The role of PTEN in the progression and survival of prostate cancer. Minerva Endocrinol. *28*, 145–153.

Dhanasekaran, S.M., Barrette, T.R., Ghosh, D., Shah, R., Varambally, S., Kurachi, K., Pienta, K.J., Rubin, M.A., and Chinnaiyan, A.M. (2001). Delineation of prognostic biomarkers in prostate cancer. Nature *412*, 822–826.

Di Cristofano, A., and Pandolfi, P.P. (2000). The multiple roles of PTEN in tumor suppression. Cell *100*, 387–390.

Di Cristofano, A., Pesce, B., Cordon-Cardo, C., and Pandolfi, P.P. (1998). Pten is essential for embryonic development and tumour suppression. Nat. Genet. *19*, 348–355.

Di Cristofano, A., De Acetis, M., Koff, A., Cordon-Cardo, C., and Pandolfi, P.P. (2001). Pten and p27KIP1 cooperate in prostate cancer tumor suppression in the mouse. Nat. Genet. *27*, 222–224.

Dubey, P., Wu, H., Reiter, R.E., and Witte, O.N. (2001). Alternative pathways to prostate carcinoma activate prostate stem cell antigen expression. Cancer Res. *61*, 3256–3261.

Dudoit, S., Yang, Y.H., Callow, M.J., and Speed, T.J. (2000). Technical report (Department of Biostatistics, University of California at Berkeley).

Fidler, I.J., and Kripke, M.L. (1977). Metastasis results from preexisting variant cells within a malignant tumor. Science *197*, 893–895.

Fidler, I.J., and Kripke, M.L. (2003). Genomic analysis of primary tumors does not address the prevalence of metastatic cells in the population. Nat. Genet. *34*, 23.

Freeman, D.J., Li, A.G., Wei, G., Li, H.H., Kertesz, N., Lesche, R., Whale, A.D., Martinez-Diaz, H., Rozengurt, N., Cardiff, R.D., et al. (2003). PTEN tumor suppressor regulates p53 protein levels and activity through phosphatase-dependent and -independent mechanisms. Cancer Cell *3*, 117–130.

Gao, X., Neufeld, T.P., and Pan, D. (2000). Drosophila PTEN regulates cell growth and proliferation through PI3K-dependent and -independent pathways. Dev. Biol. *221*, 404–418.

Garabedian, E.M., Humphrey, P.A., and Gordon, J.I. (1998). A transgenic mouse model of metastatic prostate cancer originating from neuroendocrine cells. Proc. Natl. Acad. Sci. USA *95*, 15382–15387.

Greenberg, N.M., DeMayo, F., Finegold, M.J., Medina, D., Tilley, W.D., Aspinall, J.O., Cunha, G.R., Donjacour, A.A., Matusik, R.J., and Rosen, J.M. (1995). Prostate cancer in a transgenic mouse. Proc. Natl. Acad. Sci. USA *92*, 3439–3443.

Groszer, M., Erickson, R., Scripture-Adams, D.D., Lesche, R., Trumpp, A., Zack, J.A., Kornblum, H.I., Liu, X., and Wu, H. (2001). Negative regulation of neural stem/progenitor cell proliferation by the Pten tumor suppressor gene in vivo. Science *294*, 2186–2189.

Gu, Z., Thomas, G., Yamashiro, J., Shintaku, I.P., Dorey, F., Raitano, A., Witte, O.N., Said, J.W., Loda, M., and Reiter, R.E. (2000). Prostate stem cell antigen (PSCA) expression increases with high gleason score, advanced stage and bone metastasis in prostate cancer. Oncogene *19*, 1288–1296.

Hanahan, D., and Weinberg, R.A. (2000). The hallmarks of cancer. Cell *100*, 57–70.

Harada, M., Iida, M., Yamaguchi, M., and Shida, K. (1992). Analysis of bone metastasis of prostatic adenocarcinoma in 137 autopsy cases. Adv. Exp. Med. Biol. *324*, 173–182.

He, W.W., Sciavolino, P.J., Wing, J., Augustus, M., Hudson, P., Meissner, P.S., Curtis, R.T., Shell, B.K., Bostwick, D.G., Tindall, D.J., et al. (1997). A novel human prostate-specific, androgen-regulated homeobox gene (NKX3.1) that maps to 8p21, a region frequently deleted in prostate cancer. Genomics *43*, 69–77.

Hotte, S.J., Winquist, E.W., Stitt, L., Wilson, S.M., and Chambers, A.F. (2002). Plasma osteopontin: associations with survival and metastasis to bone in men with hormone-refractory prostate carcinoma. Cancer *95*, 506–512.

Huggins, C., Stephens, R., and Hodges, C.V. (1941). Studies on prostate cancer: 2. The effects of castration on advanced carcinoma of the prostate gland. Arch. Surg. *43*, 209.

Isaacs, J.T. (1999). The biology of hormone refractory prostate cancer. Why does it develop? Urol. Clin. North Am. *26*, 263–273.

July, L.V., Akbari, M., Zellweger, T., Jones, E.C., Goldenberg, S.L., and Gleave, M.E. (2002). Clusterin expression is significantly enhanced in prostate cancer cells following androgen withdrawal therapy. Prostate *50*, 179–188.

Kasper, S., Sheppard, P.C., Yan, Y., Pettigrew, N., Borowsky, A.D., Prins, G.S., Dodd, J.G., Duckworth, M.L., and Matusik, R.J. (1998). Development, progression, and androgen-dependence of prostate tumors in probasin-large T antigen transgenic mice: a model for prostate cancer. Lab. Invest. *78*, 319–333.

Kim, M.J., Cardiff, R.D., Desai, N., Banach-Petrosky, W.A., Parsons, R., Shen, M.M., and Abate-Shen, C. (2002). Cooperativity of Nkx3.1 and Pten loss of function in a mouse model of prostate carcinogenesis. Proc. Natl. Acad. Sci. USA *99*, 2884–2889.

Kwabi-Addo, B., Giri, D., Schmidt, K., Podsypanina, K., Parsons, R., Greenberg, N., and Ittmann, M. (2001). Haploinsufficiency of the Pten tumor suppressor gene promotes prostate cancer progression. Proc. Natl. Acad. Sci. USA *98*, 11563–11568.

Landis, S.H., Murray, T., Bolden, S., and Wingo, P.A. (1999). Cancer Statistics, Vol 49. (CA: Cancer J. Clin.), 8–31.

Lesche, R., Groszer, M., Gao, J., Wang, Y., Messing, A., Liu, X., and Wu, H. (2002). Cre/loxp-mediated inactivation of the murine Pten tumor suppressor gene. Genesis *32*, 148–149.

Li, P., Lee, H., Guo, S., Unterman, T.G., Jenster, G., and Bai, W. (2003). AKT-independent protection of prostate cancer cells from apoptosis mediated through complex formation between the androgen receptor and FKHR. Mol. Cell. Biol. *23*, 104–118.

Liaw, D., Marsh, D.J., Li, J., Dahia, P.L., Wang, S.I., Zheng, Z., Bose, S., Call, K.M., Tsou, H.C., Peacocke, M., et al. (1997). Germline mutations of the PTEN gene in Cowden disease, an inherited breast and thyroid cancer syndrome. Nat. Genet. *16*, 64–67.

Lin, H.K., Wang, L., Hu, Y.C., Altuwaijri, S., and Chang, C. (2002). Phosphorylation-dependent ubiquitylation and degradation of androgen receptor by Akt require Mdm2 E3 ligase. EMBO J. *21*, 4037–4048.

Maehama, T., Taylor, G.S., and Dixon, J.E. (2001). PTEN and myotubularin: Novel phosphoinositide phosphatases. Annu. Rev. Biochem. *70*, 247–279.

Magee, J.A., Abdulkadir, S.A., and Milbrandt, J. (2003). Haploinsufficiency at the Nkx3.1 locus. A paradigm for stochastic, dosage-sensitive gene regulation during tumor initiation. Cancer Cell *3*, 273–283.

Majumder, P.K., Yeh, J.J., George, D.J., Febbo, P.G., Kum, J., Xue, Q., Bikoff, R., Ma, H., Kantoff, P.W., Golub, T.R., et al. (2003). Prostate intraepithelial neoplasia induced by prostate restricted Akt activation: the MPAKT model. Proc. Natl. Acad. Sci. USA *100*, 7841–7846.

Manin, M., Baron, S., Goossens, K., Beaudoin, C., Jean, C., Veyssiere, G., Verhoeven, G., and Morel, L. (2002). Androgen receptor expression is regulated by the phosphoinositide 3-kinase/Akt pathway in normal and tumoral epithelial cells. Biochem. J. *366*, 729–736.

Marsh, D.J., Kum, J.B., Lunetta, K.L., Bennett, M.J., Gorlin, R.J., Ahmed, S.F., Bodurtha, J., Crowe, C., Curtis, M.A., Dasouki, M., et al. (1999). PTEN mutation spectrum and genotype-phenotype correlations in Bannayan-Riley-Ruvalcaba syndrome suggest a single entity with Cowden syndrome. Hum. Mol. Genet. *8*, 1461–1472.

Masumori, N., Thomas, T.Z., Chaurand, P., Case, T., Paul, M., Kasper, S., Caprioli, R.M., Tsukamoto, T., Shappell, S.B., and Matusik, R.J. (2001). A probasin-large T antigen transgenic mouse line develops prostate adenocarcinoma and neuroendocrine carcinoma with metastatic potential. Cancer Res. *61*, 2239–2249.

Mousses, S., Bubendorf, L., Wagner, U., Hostetter, G., Kononen, J., Cornelison, R., Goldberger, N., Elkahloun, A.G., Willi, N., Koivisto, P., et al. (2002). Clinical validation of candidate genes associated with prostate cancer progression in the CWR22 model system using tissue microarrays. Cancer Res. *62*, 1256–1260.

Mundy, G.R. (2002). Metastasis to bone: causes, consequences and therapeutic opportunities. Nat. Rev. Cancer *2*, 584–593.

Nelson, P.S., Pritchard, C., Abbott, D., and Clegg, N. (2002). The human (PEDB) and mouse (mPEDB) prostate expression databases. Nucleic Acids Res. *30*, 218–220.

Podsypanina, K., Ellenson, L.H., Nemes, A., Gu, J., Tamura, M., Yamada, K.M., Cordon-Cardo, C., Catoretti, G., Fisher, P.E., and Parsons, R. (1999). Mutation of Pten/Mmac1 in mice causes neoplasia in multiple organ systems. Proc. Natl. Acad. Sci. USA *96*, 1563–1568.

Powell, W.C., Cardiff, R.D., Cohen, M.B., Miller, G.J., and Roy-Burman, P. (2003). Mouse strains for prostate tumorigenesis based on genes altered in human prostate cancer. Curr. Drug Targets *4*, 263–279.

Pritchard, C.C., Hsu, L., Delrow, J., and Nelson, P.S. (2001). Project normal: defining normal variance in mouse gene expression. Proc. Natl. Acad. Sci. USA *98*, 13266–13271.

Ramaswamy, S., Ross, K.N., Lander, E.S., and Golub, T.R. (2003). A molecular signature of metastasis in primary solid tumors. Nat. Genet. *33*, 49–54.

Reiter, R.E., Gu, Z., Watabe, T., Thomas, G., Szigeti, K., Davis, E., Wahl, M., Nisitani, S., Yamashiro, J., Le Beau, M.M., et al. (1998). Prostate stem

cell antigen: a cell surface marker overexpressed in prostate cancer. Proc. Natl. Acad. Sci. USA *95*, 1735–1740.

Sciarra, A., Mariotti, G., Gentile, V., Voria, G., Pastore, A., Monti, S., and Di Silverio, F. (2003). Neuroendocrine differentiation in human prostate tissue: is it detectable and treatable? BJU Int. *91*, 438–445.

Sellers, W.R., and Sawyers, C.L. (2002). Somatic Genetics of Prostate Cancer: Oncogenes and Tumore Suppressors (Philadelphia: Lippincott Williams & Wilkins).

Stambolic, V., Suzuki, A., de la Pompa, J.L., Brothers, G.M., Mirtsos, C., Sasaki, T., Ruland, J., Penninger, J.M., Siderovski, D.P., and Mak, T.W. (1998). Negative regulation of PKB/Akt-dependent cell survival by the tumor suppressor PTEN. Cell *95*, 29–39.

Stambolic, V., Tsao, M.S., Macpherson, D., Suzuki, A., Chapman, W.B., and Mak, T.W. (2000). High incidence of breast and endometrial neoplasia resembling human Cowden syndrome in pten+/− mice. Cancer Res. *60*, 3605–3611.

Steinberg, J., Oyasu, R., Lang, S., Sintich, S., Rademaker, A., Lee, C., Kozlowski, J.M., and Sensibar, J.A. (1997). Intracellular levels of SGP-2 (Clusterin) correlate with tumor grade in prostate cancer. Clin. Cancer Res. *3*, 1707–1711.

Sun, H., Lesche, R., Li, D.M., Liliental, J., Zhang, H., Gao, J., Gavrilova, N., Mueller, B., Liu, X., and Wu, H. (1999). PTEN modulates cell cycle progression and cell survival by regulating phosphatidylinositol 3,4,5,-trisphosphate and Akt/protein kinase B signaling pathway. Proc. Natl. Acad. Sci. USA *96*, 6199–6204.

Sun, H., Enomoto, T., Shroyer, K.R., Ozaki, K., Fujita, M., Ueda, Y., Nakashima, R., Kuragaki, C., Ueda, G., and Murata, Y. (2002). Clonal analysis and mutations in the PTEN and the K-ras genes in endometrial hyperplasia. Diagn. Mol. Pathol. *11*, 204–211.

Suzuki, A., de la Pompa, J.L., Stambolic, V., Elia, A.J., Sasaki, T., del Barco Barrantes, I., Ho, A., Wakeham, A., Itie, A., Khoo, W., et al. (1998a). High cancer susceptibility and embryonic lethality associated with mutation of the PTEN tumor suppressor gene in mice. Curr. Biol. *8*, 1169–1178.

Suzuki, H., Freije, D., Nusskern, D.R., Okami, K., Cairns, P., Sidransky, D., Isaacs, W.B., and Bova, G.S. (1998b). Interfocal heterogeneity of PTEN/MMAC1 gene alterations in multiple metastatic prostate cancer tissues. Cancer Res. *58*, 204–209.

Tanaka, M., Komuro, I., Inagaki, H., Jenkins, N.A., Copeland, N.G., and Izumo, S. (2000). Nkx3.1, a murine homolog of Drosophila bagpipe, regulates epithelial ductal branching and proliferation of the prostate and palatine glands. Dev. Dyn. *219*, 248–260.

Thalmann, G.N., Sikes, R.A., Devoll, R.E., Kiefer, J.A., Markwalder, R., Klima, I., Farach-Carson, C.M., Studer, U.E., and Chung, L.W. (1999). Osteopontin: possible role in prostate cancer progression. Clin. Cancer Res. *5*, 2271–2277.

Tusher, V.G., Tibshirani, R., and Chu, G. (2001). Significance analysis of microarrays applied to the ionizing radiation response. Proc. Natl. Acad. Sci. USA *98*, 5116–5121.

van 't Veer, L.J., Dai, H., van de Vijver, M.J., He, Y.D., Hart, A.A., Mao, M., Peterse, H.L., van der Kooy, K., Marton, M.J., Witteveen, A.T., et al. (2002). Gene expression profiling predicts clinical outcome of breast cancer. Nature *415*, 530–536.

Vivanco, I., and Sawyers, C.L. (2002). The phosphatidylinositol 3-Kinase AKT pathway in human cancer. Nat. Rev. Cancer *2*, 489–501.

Wang, J.Y., Huang, T.J., Chen, F.M., Hsieh, M.C., Lin, S.R., Hou, M.F., and Hsieh, J.S. (2003). Mutation analysis of the putative tumor suppressor gene PTEN/MMAC1 in advanced gastric carcinomas. Virchows Arch. *442*, 437–443.

Weng, L., Brown, J., and Eng, C. (2001). PTEN induces apoptosis and cell cycle arrest through phosphoinositol-3-kinase/Akt-dependent and -independent pathways. Hum. Mol. Genet. *10*, 237–242.

Wu, X., Senechal, K., Neshat, M.S., Whang, Y.E., and Sawyers, C.L. (1998). The PTEN/MMAC1 tumor suppressor phosphatase functions as a negative regulator of the phosphoinositide 3-kinase/Akt pathway. Proc. Natl. Acad. Sci. USA *95*, 15587–15591.

Wu, X., Wu, J., Huang, J., Powell, W.C., Zhang, J., Matusik, R.J., Sangiorgi, F.O., Maxson, R.E., Sucov, H.M., and Roy-Burman, P. (2001). Generation of a prostate epithelial cell-specific Cre transgenic mouse model for tissue-specific gene ablation. Mech. Dev. *101*, 61–69.

You, M.J., Castrillon, D.H., Bastian, B.C., O'Hagan, R.C., Bosenberg, M.W., Parsons, R., Chin, L., and DePinho, R.A. (2002). Genetic analysis of Pten and Ink4a/Arf interactions in the suppression of tumorigenesis in mice. Proc. Natl. Acad. Sci. USA *99*, 1455–1460.

Zhou, X.P., Loukola, A., Salovaara, R., Nystrom-Lahti, M., Peltomaki, P., de la Chapelle, A., Aaltonen, L.A., and Eng, C. (2002). PTEN mutational spectra, expression levels, and subcellular localization in microsatellite stable and unstable colorectal cancers. Am. J. Pathol. *161*, 439–447.